

1 **Liver Echinococcosis Lesion Classification Tool by**  
2 **Deep Learning: development, deployment, and**  
3 **validations**

4 Liang Huang<sup>1</sup>, Xiaohong Xi<sup>2</sup>, Zhu Chen<sup>1</sup>, Yilan Zeng<sup>1</sup>

5 <sup>1</sup>Chengdu Public Health Clinical Center, Chengdu City, Sichuan Province, China,

6 61000

7 <sup>2</sup>Department of Sonography, Chenghua Women and Children's Hospital, Chengdu

8 City, Sichuan Province, China, 61000

9

10 Correspondence:

11 Yilan Zeng, Chengdu Public Health Clinical Center, 377 Jingming Road, Chengdu

12 City, Sichuan Province, China (hyuangx@qq.com).

13

14

15

16

17

18

19

20

21

22

## 23 Abstract

24 The endemic of Echinococcosis imposed heavy disease burden in some areas. The  
25 sonography for Echinococcosis lesions was essential to disease diagnosis and  
26 managements. Especially the biological typing of lesions was key to disease  
27 treatments. We used deep-learning tools to help sonographer to classify the lesion  
28 types. The model achieved 85%(302/376) accuracy, in contrast to senior sonographer  
29 achieved 72%(61/85) accuracy. The accuracy of AI model was higher than senior  
30 sonographer (p-value=0.01), could be a feasible method to help sonographer in  
31 remote area.

32

33

34

35

36

37

38

39

## 40 **Introduction**

41 Echinococcosis is a result of human infection by larval stages of taeniid cestodes of  
42 the genus *Echinococcus*. *Echinococcus granulosus* causes cystic echinococcosis(CE),  
43 *Echinococcus multilocularis* causes alveolar echinococcosis (AE), two separately  
44 diseases with different biological processes<sup>1,2</sup>. The co-infection of the two pathogens  
45 was rare<sup>3</sup>. At least 58% of the population are at risk of acquiring echinococcosis,  
46 distributed in Europe, North and Central America, Africa, Australia and Western  
47 China<sup>4</sup>. It is a potential fatal zoonosis<sup>5</sup>, a major public health concern in  
48 Qinghai-Tibet Plateau due to the highly pandemic of both CE and AE. The  
49 echinococcosis DALYs in the Tibetan communities were 126,159 life years annually  
50 estimated by Wang<sup>6</sup>. The Tibet population in China holds 1.66% prevalence of both  
51 CE and AE, estimated 50 million people are at risk of infecting the disease in Western  
52 China<sup>7</sup>. China has been investing large amount of resources to control echinococcosis,  
53 launched national control program<sup>8</sup>. The strategies of the national control program  
54 majorly included definitive hosts deworming, slaughtering control, and intermediate  
55 hosts vacation<sup>2</sup>. Ultrasound screening was included as an essential measure to find the  
56 patients and follow-up.

57 Echinococcosis is chronic parasites disease, liver echinococcosis were most common  
58 in clinical<sup>9</sup>. The treatments for it included surgically remove the lesion,  
59 PAIR(puncture, aspiration, injection, and respiration), albendazole or they

60 combined<sup>10,2</sup>. The lesion classification for CE is the one of the key aspects in patients'  
61 management, since the classification was closely correlated to the underlying  
62 biological status of the larva.

63 For CE, the ultrasonic WHO classification is commonly used (CL, CE1, CE2, CE3,  
64 CE4, and CE5). The CE1-2 types of CE indicating active infection should be treated  
65 by Albendazole or/and surgical resection. The CE4-5 are considered degenerated  
66 lesion due to failure of natural infection or effects of treatments, should be closely  
67 monitored<sup>11,12</sup>. The CE3 is considered the transitional phase of lesion. The CE1-5 are  
68 the continuous progress of “active-transitional-inactive”<sup>13</sup> indicating importance for  
69 biological process and disease assessments.

70 The AE is a silent progressing infiltrative proliferation of the parasite, mimicking a  
71 malignancy<sup>14</sup>. For AE cases, the lesion classification are more complex and uncertain,  
72 research revealed that the clinical stage of AE was not correlated to ultrasound  
73 appearance<sup>15</sup>. WHO had proposed a PNM classification system for AE<sup>16</sup>. The PNM  
74 classification system (P=parasitic mass in the liver, N=involvement of neighboring  
75 organs, and M=metastasis) was designed to systematic evaluation for surgical purpose  
76 majorly. Besides PNM classification system, the Ulm university proposed a  
77 classification system for AE<sup>17</sup>, and five types of lesion proposed.

78 The PNM classification systems required extra examinations other than ultrasound,  
79 such as CT or MRI scan. However, the PNM system was not feasible for many

80 occasions. The accessibility of medical resources in Qinghai-Tibet Plateau is  
81 incomparable with urban area<sup>18</sup> due to the high altitude and atrocious weather, the  
82 local paramedics are lack of professional training, especially for sonography.

83 This study purposed to develop deep learning-based application to automatically type  
84 lesions for both AE and CE, giving diagnostic assistant for local paramedics. In this  
85 study, we used 2820 ultrasound images training our model, and used external data to  
86 validate the model. It is the largest echinococcosis ultrasound training set so far and  
87 its application for was published on a web for open access.

88 Previous studies had developed deep learning system for hepatology by using medical  
89 images, pathology, clinical and laboratory data, natural languages, etc. They are  
90 majorly designed to address liver problems such as liver fibrosis(cirrhosis), liver  
91 cancer, portal hypotension, etc<sup>19</sup>. Relatively, less study were aimed to the liver  
92 echinococcosis, which is on the list of NZDs<sup>20</sup> by WHO. Before our study, Xin had  
93 built a segmentation and classification networks for echinococcosis, shedding light on  
94 potential development in this field. However, it used 160 CT scan images for training,  
95 and the classification of echinococcosis were not covered all types of both AE and  
96 CE<sup>21</sup>. Comparing with CT images, ultrasound was more widely used in filed  
97 echinococcosis diagnosis. In this study, we used 2820 ultrasound images for training  
98 covering all echinococcosis types.

## 99 **Method and Material**

100 **Patient Data**

101 Sonographies were retrospectively obtained from National Control Program for  
102 Echinococcosis Screening in Qinghai-Tibet Plateau<sup>22</sup>. The medical decisions were not  
103 based on results of this study. All the patients were previously diagnosed  
104 echinococcosis by systematic evaluations including medical images and serology tests,  
105 fulfilled the criteria of echinococcosis diagnosis criteria.

106 In this study, we collected 3423 images of echinococcosis patients who were enrolled  
107 and routinely managed in national echinococcosis control program.

108 Ethical approval for this retrospective study was obtained from the Ethics Committee  
109 of the Chengdu Public Health Clinical Center. The patient consents for inclusion were  
110 waived as the retrospective nature of this study and anonymous data use.

111

112 **Classification criteria**

113 In this study, we used CL-CE5 classification system for CE, which was recommended  
114 by WHO recommendation<sup>13</sup>. We used infiltrating, calcification, and necrotic lesion  
115 for AE classification, which was recommended by Chinses Guideline for AE<sup>23</sup>.

116 For CE lesions, the CL lesion, which was appears “cystic lesion”, which appears no  
117 different from simple cyst in liver, could not be confirmed by ultrasound image solely.

118 The CE1 refers to a simple round or oval unilocular cyst with anechoic content and a  
119 visible double cystic wall. The CE2 cyst is filled with daughter vesicles. The CE3

120 cysts includes two stages, CE3a is characterized by the “water-lily” sign, CE3b  
121 represented by floating membranes. The CE4 typically reveals coarse variable  
122 hyperechogenic or hypoechogenic echotexture without daughter vesicles. The “ball of  
123 wool” sign, corresponding to the detached endocyst as a hypoechoic folded structure  
124 embedded in a hyperechoic matrix, is the key ultrasound sign. The CE5 cysts are  
125 partially (with an egg-shell calcified wall) or completely calcified with shadowing<sup>13</sup>.

126 For AE lesions, in this study, we followed the Chinese Guideline for AE, which was  
127 also applied in National Controlling Program in endemic areas. It proposed three  
128 ultrasound types of lesions. The infiltrative lesion (AE1) appearing hailstorm pattern,  
129 heterogeneously echogenic areas, in many cases scatter calcifications can be seen.  
130 The necrosis lesion (AE2), appearing a pseudocystic pattern with an irregular  
131 hyperechoic rim. The calcification lesion, appearing solid hyperechoic lesion (AE3).

### 132 **Data labelling**

133 Expert who had more than 15 years of echinococcosis ultrasound diagnosis and  
134 ultrasound based echinococcosis patients managements had labeled the included  
135 ultrasound images by using LabelMe<sup>24</sup>, an open-source image label tool. The lesions  
136 in the images were labeled by different color, and normal liver background was  
137 labeled as black. The labeled images were automatically cropped into fixed size of  
138 input images (512\*512 pixels) for model learning and inference.

139 **Model constructions**

140 The U-net architecture achieves high performance on different biomedical images  
141 segmentation applications by using relatively less quantity of training images<sup>25,26</sup>. In  
142 this study, we used two separated U-net models. Firstly, we constructed “Classifier”  
143 U-net model which was used generalized multiclass dice loss (GMD). The GMD  
144 penalizes the wrong classifications more aggressively and more effective for training  
145 if the unbalanced category of training samples used. However, it produces more noise  
146 (false positive predictions) produced. Secondly, the identical “Shaper” U-net using  
147 conventional binary dice loss function focusing on lesion shape learning black-white  
148 (lesion-background, values 0 and 1) outputs, omitting the lesion class information. It  
149 produced more accurate shape inference for lesions. The inference result produced by  
150 multiplication of two tensors of the models’ outputs (Figure 1).

151 The whole program was based on Python programming languages with PyTorch 1.3  
152 deep learning framework. The core construction of the models consist 10 of  
153 convectional layers including downsampling, upsampling, and attention gates were  
154 used in this model<sup>27</sup>. The models were trained with mini-batch SGD optimizer with  
155 momentum on two Nvidia 1080TI GPUs. The learning rate was chosen to minimize  
156 the error in the tuning dataset. Early stop training strategies was used for preventing  
157 over fitting.

158 **Web-based user interface**



159 Trained weights files loaded in a web-based user interface under Flask framework for  
160 internal logical process and HTML for appearances of the application of both  
161 computer and mobile phone. The users will upload images transferred from  
162 ultrasound equipment by computer or mobile phone. The web-based UI will  
163 automatically calculate the hot-spot of the ultrasound images and crop them into  
164 proper size and optimized location(Figure 2).

### 165 **Model validations**

166 We compared classification accuracies for human and model. The senior sonographer  
167 has 15 years of working experiences. The performance of model was designed to  
168 achieved equivalent accuracy with senior sonographer.

### 169 **Statistical analysis**

170 The statistical analysis was performed with the STATA/SE 14.1 software (StataCorp ,  
171 4905 Lakeway Drive, College Station, Texas , USA) and R 4.0.2<sup>28</sup>. The ggplot2<sup>29</sup> for  
172 R was used for diagram plotting. Confusion matrix<sup>30</sup> was used for validation of the  
173 accuracy of the model. The confusion matrix was plotted by ggplot2 packages. The  $\alpha$   
174 was set to 0.05.  $P < \alpha$  was statistically significant.

### 175 **Hardware and software**

176 The sonographies were obtained from various ultrasound equipment, including  
177 Mindray™ M5, Seote MyLab™ Alpha. The server used for training model installed

178 two 1080TI GPUs with Ubuntu 18.04 LTS platform. A Nvidia AGX Xavier edge  
179 computing device providing web-based interface and model inference. These devices  
180 install Ubuntu 18.04 LTS with PyTorch 1.3 and Flask library installed.

## 181 **Result**

### 182 **Dataset**

183 According to our dataset, we had 2250 training images, 190 images validation images  
184 and 376 testing images. In the training dataset, for CL and CE1-5 type, 140, 172, 198,  
185 280, and 472 images were trained, respectively. For AE lesion, 420, 290, and 278  
186 images were trained, respectively.

### 187 **Training the model and publishing**

188 Model was trained for about 10 hours to achieved convergence after 90 epochs  
189 (multiple times of training for optimizing). The generalized dice score of Classifier  
190 for validation set was 0.77, the Dice score of Shaper for validation set was, 0.86. The  
191 web-based interface uses 3.1s for average for single image analysis in current  
192 hardware configuration (each service has six times of inferences).

### 193 **Comparison with human sonographer**

194 Total of 376 samples were inputted into AI model, archived 85%(302/376) accuracy.  
195 In contrast, total of 85 samples were classified by senior sonographer achieved

196 72%(61/85) accuracy. The accuracy of AI model was higher than senior sonographer

197 (p-value=0.01 by chi-square test)(Table 1).

198 However, the difference for each types of lesions were not statically significant

199 (except CE5, the human sonographer achieved extremely low accuracy). The result

200 were represented as confusion matrix(Figure 3 and Figure 4).

## 201 **Discussion**

### 202 **Model outperforms trained sonographers**

203 According to our testing, our deep learning model outperformed fast-trained

204 sonographer in echinococcosis classification task. The U-net based model has been

205 proven to be efficient for smaller size of training set. It could be highly useful for

206 local paramedics while managing echinococcosis patients.

### 207 **Background of the disease**

208 *Echinococcus granulosus* life cycle involves dogs and other canids as definitive hosts

209 for the intestinal tapeworm as intermediate hosts for metacestode (larval) stage. The

210 metacestode (echinococcal cyst). In humans, the slowly growing hydatid cysts can

211 attain a volume of several liters and contain many thousands of protoscolices<sup>31</sup>.

212 The life cycle of *E. multilocularis* involves small rodent intermediate hosts, such as

213 arvicolid, wild or domestic canid definitive hosts, such as red or arctic foxes, jackals,

214 wolves, or dogs. Humans are aberrant intermediate hosts acquiring the infection

215 through ingestion of eggs shed in the feces of definitive hosts. AE is of increasing  
216 concern globally due to the geographical spread of the parasite, its increasing  
217 prevalence in animals from endemic areas, the absence of a vaccine, and the lack of  
218 active control measures to prevent the infection<sup>32</sup>.

## 219 **Web-based application improved accessibility of AI** 220 **tools**

221 Deep learning applications are provided as source code deposited on Github<sup>33</sup> or  
222 similar platform for sharing. It is not feasible for many medical related applications,  
223 since the privacy concern of the data. The run-time environments of the source code  
224 were varied in wide range due to different platforms, different frameworks, and  
225 versions used. Here we used open-access web-based tool available for PC and mobile  
226 will significantly increase the accessibility for many remote areas.

## 227 **Clinical implications**

228 We demonstrated the AI model achieved better performance than sonographer, it  
229 could help doctors in remoted area for echinococcosis lesion typing. The lesion typing  
230 for echinococcosis was important for disease managements.

231 According to the consensus on cystic echinococcosis diagnosis and treatment, five  
232 types of lesions were recommended for classification. A natural grouping of the cysts  
233 into three relevant groups: active (CE1 and 2), transitional (CE3) and inactive (CE4

234 and 5). The lesion classification is critical to patients managements, according to the  
235 consensus, CE4 and 5 indicated an inactive infection, watch and wait was  
236 recommended, if patients with CE1-3, the consensus suggested an active larva  
237 infection, radical medical surgery or/and ABZ should be suggested<sup>11,2</sup>.

238 Comparing CE, AE is more problematic, surgical resection, chemotherapy, early  
239 diagnosis, and multidisciplinary discussion contributed to the successful treatment for  
240 AE cases<sup>11</sup>. AE lesions behave “cancer-like”<sup>34</sup>, radical surgery is the first choice in all  
241 cases suitable for totally resection<sup>11</sup>. Benzimidazoles should be used for all cases<sup>11</sup>,  
242 and liver transplantation as an alternative to palliative surgery, however, has not been  
243 shown to be superior to long-term conservative therapy<sup>35</sup>.

244

245

- 246 1. Moro, P. & Schantz, P. M. Echinococcosis: a review. *Int. J. Infect. Dis.* **13**,  
247 125–133 (2009).
- 248 2. Wen, H. *et al.* Echinococcosis: Advances in the 21st Century. *Clin. Microbiol.*  
249 *Rev.* **32**, e00075-18, /cmr/32/2/CMR.00075-18.atom (2019).
- 250 3. Wang, X. Q., Han, X. M., Tian, Q. S., Zhao, S. Y. & A, J. D. [Hepatic cystic and  
251 alveolar echinococcosis co-infections: a report of 3 cases]. *Zhongguo Xue Xi Chong*  
252 *Bing Fang Zhi Za Zhi Chin. J. Schistosomiasis Control* **32**, 213–216 (2019).
- 253 4. Deplazes, P. *et al.* Global Distribution of Alveolar and Cystic Echinococcosis. in  
254 *Advances in Parasitology* vol. 95 315–493 (Elsevier, 2017).
- 255 5. Guo, B. *et al.* High endemicity of alveolar echinococcosis in Yili Prefecture,  
256 Xinjiang Autonomous Region, the People’s Republic of China: Infection status in  
257 different ethnic communities and in small mammals. *PLoS Negl. Trop. Dis.* **15**,  
258 e0008891 (2021).
- 259 6. Wang, Q. *et al.* Disease burden of echinococcosis in Tibetan communities—A  
260 significant public health issue in an underdeveloped region of western China. *Acta*  
261 *Trop.* **203**, 105283 (2020).

- 262 7. Shan, X. *et al.* Health-related quality of life (HRQoL) associated with  
263 echinococcosis patients in Tibetan communities in Shiqu County, China: a  
264 case-control study. *Qual. Life Res.* **29**, 1559–1565 (2020).
- 265 8. Nationa echinococcosis Control programe(in Chinese).  
266 [http://www.gov.cn/zhengce/zhengceku/2020-09/03/content\\_5539743.htm](http://www.gov.cn/zhengce/zhengceku/2020-09/03/content_5539743.htm).
- 267 9. Eckert, J. & Deplazes, P. Biological, Epidemiological, and Clinical Aspects of  
268 Echinococcosis, a Zoonosis of Increasing Concern. *Clin. Microbiol. Rev.* **17**, 107–135  
269 (2004).
- 270 10. Gupta, N. *et al.* Hepatic Hydatid: PAIR, Drain or Resect? *J. Gastrointest. Surg.*  
271 **15**, 1829–1836 (2011).
- 272 11. Brunetti, E., Kern, P. & Vuitton, D. A. Expert consensus for the diagnosis and  
273 treatment of cystic and alveolar echinococcosis in humans. *Acta Trop.* **114**, 1–16  
274 (2010).
- 275 12. Larrieu, E. *et al.* Epidemiology, diagnosis, treatment and follow-up of cystic  
276 echinococcosis in asymptomatic carriers. *Trans. R. Soc. Trop. Med. Hyg.* **113**, 74–80  
277 (2019).
- 278 13. Brunetti, E. *et al.* Ultrasound and Cystic Echinococcosis. *Ultrasound Int. Open*  
279 **04**, E70–E78 (2018).
- 280 14. Casulli, A., Barth, T. F. E. & Tamarozzi, F. Echinococcus multilocularis. *Trends*  
281 *Parasitol.* **35**, 738–739 (2019).
- 282 15. Sulima, M. *et al.* Ultrasound images in hepatic alveolar echinococcosis and  
283 clinical stage of the disease. *Adv. Med. Sci.* **64**, 324–330 (2019).
- 284 16. Kern, P. *et al.* WHO classification of alveolar echinococcosis: Principles and  
285 application. *Parasitol. Int.* **55**, S283–S287 (2006).
- 286 17. Kratzer, W. Proposal of an ultrasonographic classification for hepatic alveolar  
287 echinococcosis: Echinococcosis multilocularis Ulm classification-ultrasound. *World J.*  
288 *Gastroenterol.* **21**, 12392 (2015).
- 289 18. Yang, S.-J. *et al.* A remote management system for control and surveillance of  
290 echinococcosis: design and implementation based on internet of things. *Infect. Dis.*  
291 *Poverty* **10**, 50 (2021).
- 292 19. Ahn, J. C., Connell, A., Simonetto, D. A., Hughes, C. & Shah, V. H. The  
293 application of artificial intelligence for the diagnosis and treatment of liver diseases.  
294 *Hepatol. Baltim. Md* (2020) doi:10.1002/hep.31603.
- 295 20. Borhani, M. *et al.* Cystic echinococcosis in the Eastern Mediterranean region:  
296 Neglected and prevailing! *PLoS Negl. Trop. Dis.* **14**, e0008114 (2020).
- 297 21. Xin, S. *et al.* Automatic lesion segmentation and classification of hepatic  
298 echinococcosis using a multiscale-feature convolutional neural network. *Med. Biol.*  
299 *Eng. Comput.* **58**, 659–668 (2020).
- 300 22. Yu, Q., Xiao, N., Han, S., Tian, T. & Zhou, X.-N. Progress on the national  
301 echinococcosis control programme in China: analysis of humans and dogs population  
302 intervention during 2004–2014. *Infect. Dis. Poverty* **9**, 137 (2020).

- 303 23. Sichuan Institute of Echinococcosis Clinical Research. Guide line for complex  
304 alveolar echinococcosis. *Chin. J. Bases Clin. Gen. Surg.* **27**, 18 (23).
- 305 24. Kentaro, W. *labelme: Image Polygonal Annotation with Python*. (2016).
- 306 25. U-Net: Convolutional Networks for Biomedical Image Segmentation.  
307 <https://lmb.informatik.uni-freiburg.de/people/ronneber/u-net/>.
- 308 26. Ronneberger, O., Fischer, P. & Brox, T. U-Net: Convolutional Networks for  
309 Biomedical Image Segmentation. in *Medical Image Computing and*  
310 *Computer-Assisted Intervention – MICCAI 2015* (eds. Navab, N., Hornegger, J.,  
311 Wells, W. M. & Frangi, A. F.) vol. 9351 234–241 (Springer International Publishing,  
312 2015).
- 313 27. Oktay, O. *et al.* Attention U-Net: Learning Where to Look for the Pancreas.  
314 *ArXiv180403999 Cs* (2018).
- 315 28. *R Core Team* (2020). *R: A language and environment for statistical computing*. *R*  
316 *Foundation for Statistical Computing, Vienna, Austria*. URL  
317 <https://www.R-project.org/>.
- 318 29. Hadley, W. *ggplot2: Elegant Graphics for Data Analysis*. (Springer-Verlag New  
319 York, 2016).
- 320 30. Foody, G. M. Status of land cover classification accuracy assessment. *Remote*  
321 *Sens. Environ.* **80**, 185–201 (2002).
- 322 31. Moro, P. & Schantz, P. M. Echinococcosis: a review. *Int. J. Infect. Dis.* **13**,  
323 125–133 (2009).
- 324 32. Casulli, A., Barth, T. F. E. & Tamarozzi, F. Echinococcus multilocularis. *Trends*  
325 *Parasitol.* **35**, 738–739 (2019).
- 326 33. GitHub: Where the world builds software · GitHub. <https://github.com>.
- 327 34. Reinehr, M. *et al.* Pathology of Echinococcosis: A Morphologic and  
328 Immunohistochemical Study on 138 Specimens With Focus on the Differential  
329 Diagnosis Between Cystic and Alveolar Echinococcosis. *Am. J. Surg. Pathol.* **44**,  
330 43–54 (2020).
- 331 35. Salm, L. A., Lachenmayer, A., Perrodin, S. F., Candinas, D. & Beldi, G. Surgical  
332 treatment strategies for hepatic alveolar echinococcosis. *Food Waterborne Parasitol.*  
333 **15**, e00050 (2019).

334

335

336

337 Table 1. Comparison of human and AI

338

	CL	CE1	CE2	CE3	CE4	CE5	AE1	AE2	AE3	total	acc.*	p-values#
CL-Human	2	2	0	0	0	0	0	0	0	4	0.50	0.27
CL-AI	38	4	4	0	4	0	0	0	0	50	0.76	
CE1-Human	1	11	0	0	0	0	0	0	0	12	0.92	0.68
CE1-AI	4	40	4	0	2	0	0	0	0	50	0.80	
CE2-Human	0	0	2	1	0	0	0	0	0	3	0.67	1.00
CE2-AI	0	0	38	9	3	0	0	0	0	50	0.76	
CE3-Human	0	0	2	8	1	0	0	0	0	11	0.73	1.00
CE3-AI	0	0	6	38	6	0	0	0	0	50	0.76	
CE4-Human	0	0	0	1	14	7	0	0	0	22	0.64	0.15
CE4-AI	0	0	8	2	40	0	0	0	0	50	0.80	
CE5-Human	1	0	0	0	2	0	1	0	0	4	0.00	0.00
CE5-AI	0	1	0	0	1	40	8	0	0	50	0.80	
AE1-Human	0	0	0	0	2	0	19	0	0	21	0.90	0.21
AE1-AI	0	0	0	0	0	0	49	0	1	50	0.98	
AE2-Human	0	0	0	0	0	0	1	3	0	4	0.75	1.00
AE2-AI	0	2	0	0	0	0	2	10	0	14	0.71	
AE3-Human	0	0	0	0	0	1	1	0	2	4	0.50	0.55
AE3-AI	0	0	0	0	0	2	1	0	9	12	0.75	

339

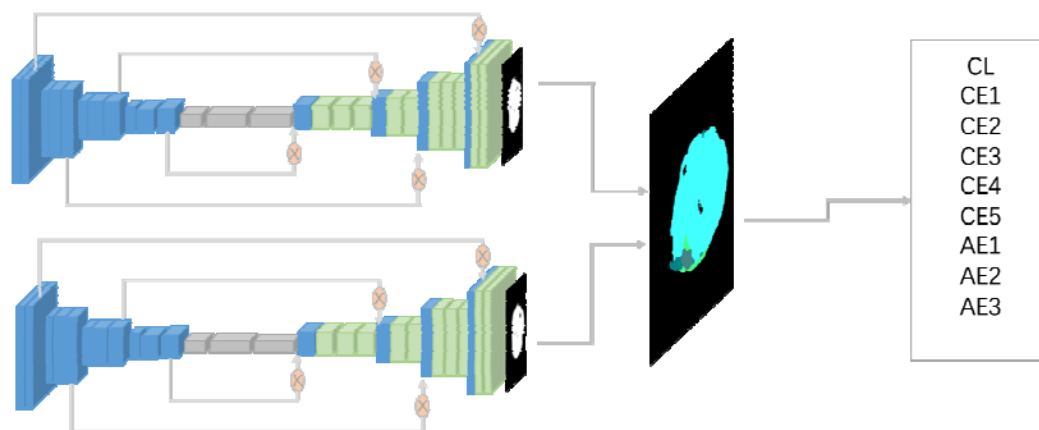
\* acc. accuracy=right classification/total samples



340 # by using Fisher' exact tests.

341

342

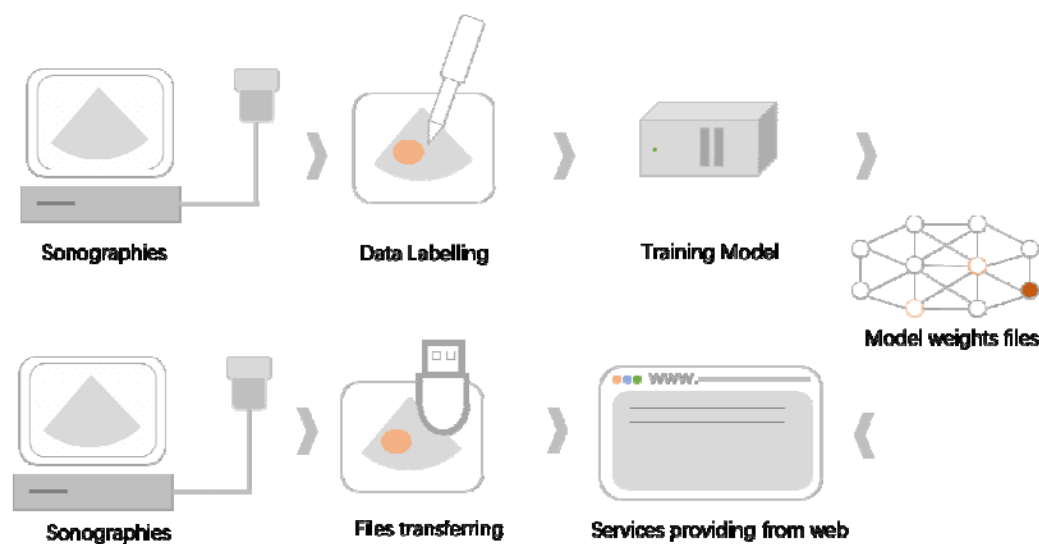


343

344 Figure 1. The architecture of Two U-nets model.

345

346



347

348 Figure 2. Web Application structure of model

349

350

351

352

353

354

355

356

357

358

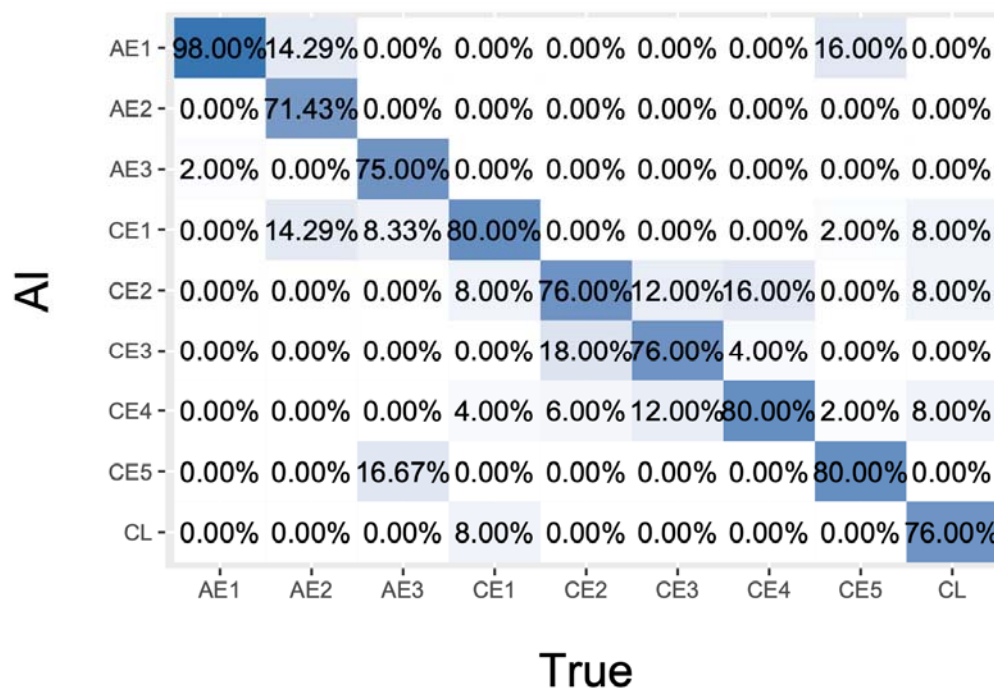
359

360

361

362  
 363  
 364  
 365  
 366  
 367  
 368  
 369

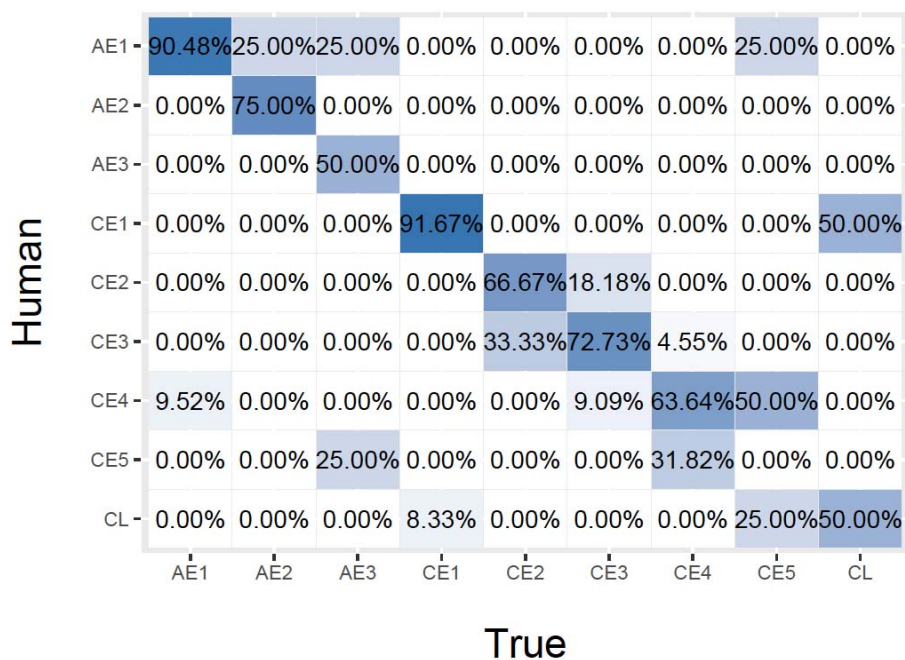
Figure 3.



370  
 371 The confusion matrix of AI prediction.  
 372  
 373  
 374  
 375  
 376  
 377  
 378  
 379  
 380  
 381  
 382  
 383  
 384  
 385  
 386

387  
388  
389  
390  
391  
392  
393  
394  
395

Figure 4.



396  
397  
398

The confusion matrix of human sonographer.